SANDIA REPORT

SAND2021-11437

Printed Click to enter a date

Sandia National Laboratories

Quantum Sensed Electron Spin Resonance Discovery Platform Final Report

Michael Lilly, Maziar Saleh Ziabari, Michael Titze, Jacob Henshaw, Ed Bielejec, Dale Huber, Andrew Mounce

Prepared by
Sandia National Laboratories
Albuquerque, New Mexico
87185 and Livermore,
California 94550

Issued by Sandia National Laboratories, operated for the United States Department of Energy by National Technology & Engineering Solutions of Sandia, LLC.

Available to DOE and DOE contractors from

U.S. Department of Energy

Office of Scientific and Technical Information

P.O. Box 62

Oak Ridge, TN 37831

Telephone: (865) 576-8401

Facsimile: (865) 576-5728

E-Mail: reports@osti.gov

Online ordering: http://www.osti.gov/scitech

Available to the public from

U.S. Department of Commerce

National Technical Information Service

5301 Shawnee Rd

Alexandria, VA 22312

Telephone: (800) 553-6847

Facsimile: (703) 605-6900

E-Mail: orders@ntis.gov

Online order: https://classic.ntis.gov/help/order-methods/

ABSTRACT

The properties of materials can change dramatically at the nanoscale new and useful properties can emerge. An example is found in the paramagnetism in iron oxide magnetic nanoparticles. Using magnetically sensitive nitrogen-vacancy centers in diamond, we developed a platform to study electron spin resonance of nanoscale materials. To implement the platform, diamond substrates were prepared with nitrogen vacancy centers near the surface. Nanoparticles were placed on the surface using a drop casting technique. Using optical and microwave pulsing techniques, we demonstrated T1 relaxometry and double electron-electron resonance techniques for measuring the local electron spin resonance. The diamond NV platform developed in this project provides a combination of good magnetic field sensitivity and high spatial resolution and will be used for future investigations of nanomaterials and quantum materials.

ACKNOWLEDGEMENTS

This work was performed, in part, at the Center for Integrated Nanotechnologies, an Office of Science User Facility operated for the U.S. Department of Energy (DOE) Office of Science. Sandia National Laboratories is a multimission laboratory managed and operated by National Technology & Engineering Solutions of Sandia, LLC, a wholly owned subsidiary of Honeywell International, Inc., for the U.S. DOE's National Nuclear Security Administration under contract DE-NA-0003525. The views expressed in the article do not necessarily represent the views of the U.S. DOE or the United States Government.

CONTENTS

LIST OF FIGURES

This page left blank

ACRONYMS AND DEFINITIONS

Abbreviation	Definition
CCD	Charge coupled device element for image acquisition
DEER	Double electron-electron resonance
ESR	Electron spin resonance
NMR	Nuclear magnetic resonance
NV	Nitrogen vacancy color center
NV0	Neutral NV color center
NV-	Negatively charged NV color center (for magnetometry)
ODMR	Optically detected magnetic resonance
PL	Photoluminescence
SEM	Scanning electron microscope
SPION	Superparamagnetic iron oxide nanoparticle
T1	Spin lifetime
T2	Spin coherence time

1. BACKGROUND

The physical properties of materials can change dramatically as the size is reduced, and at the nanoscale new and useful properties can emerge. For magnetic systems at large length scales, the magnetization is hysteretic with the applied magnetic field. As the length scale is reduced, nanoscale magnetic materials can exhibit superparamagnetism. The energy to reorient the domain can be smaller than the thermal energy, so averaged over time the net magnetization at zero field can be zero, but the susceptibility, or ability to magnetize the particle with a field, can be strong like a ferromagnet. One example of a nanoscale magnetic system is superparamagnetic iron oxide nanoparticles (SPIONs) [1]. These particles are of interest as contrast agents for magnetic resonance imaging (MRI), as magnetic materials for circuit elements and have been proposed as an approach for early detection of cancer. Due to the small size of the nanoparticles, magnetic characterization techniques often require a large number of nanoparticles. In order to more directly access the quantum properties of nanomaterials, we need to extend existing characterization techniques to the probe the discrete behavior and interactions between particles more directly. In this project, we developed a platform to measure local magnetic fields using nitrogen-vacancy (NV) centers in diamond, and these approaches enable dc (for static fields) and ac (for spin resonance) magnetic field measurements.

Nitrogen-vacancy (NV) color centers can be used as extremely sensitive magnetic field detectors [2,3]. Low energy ion implantation of N into diamond creates NV color centers near the surface of the diamond where they can be used to remotely sense the local magnetic fields. Placing a nanomaterial close to the NVs at the surface of the diamond gives us a new platform for using quantum sensing techniques to detect magnetic fields in nearby materials. To use this approach for SPIONs, we place a layer of nanoparticles on the surface of the diamond with a shallow NV layer for sensing. In a magnetic field, unpaired electrons will rotate at the Larmor frequency, and the electron spins can be controlled with microwaves. Optical and microwave techniques enable initialization and read out of the NVs and measurement of the local magnetic field. Using double electron-electron resonance (DEER) and T1 relaxometry, a target population of spins, for example the spin of nearby nanoparticles, is probed.

Magnetic resonance techniques provide some of the most versatile characterization tool of both chemical and physical materials. Nuclear magnetic resonance (NMR) is sensitive to chemical spectra due to specific radio-frequency resonances that can be used to identify both composition and the internal chemical structure. Electron spin resonance (ESR) occurs in the microwave regime and can be used in materials such as magnetic nanoparticles with unpaired electrons. ESR is sensitive to spin waves, spin dynamics, electronic or magnetic interactions, and low energy excited states of quantum systems. ESR results for iron nanoparticles in suspension are shown in Figure 1(b) for several nanoparticle concentrations [4]. There are two notable features: a sharp feature at 3400 gauss for low concentration, and a broader response for higher concentration. For an x-band resonator (9.8GHz), the sharp feature at ~3400 gauss responds like a bare electron. The broader response at higher magnetic nanoparticle concentration is due to long range dipole interactions and clustering of nanoparticles. Because the response is from an ensemble of nanoparticles, magnetic interactions between individual nanoparticles cannot be directly measured.

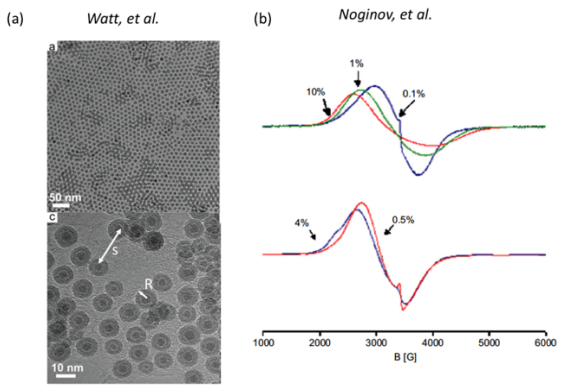

Figure 1(a) Iron oxide nanoparticles [5]. (b) ESR results [6] in a solid (upper right) and liquid (lower right) suspensions. The sharp feature at 3300 gauss for low concentrations has g=2 like an electron. The broad ESR response from 2000-4000 gauss is due to long range interaction between nanoparticles.

1.1. Objectives and outcomes

The key objectives for this project are to build a quantum sensing electron spin resonance platform using NV color centers in diamond. Section 2 covers the design of the diamond with NV color centers and the integration of nanoparticles. In Section 3, the techniques for using NV color centers for magnetometry are described. Challenges with detecting ESR in SPIONs are discussed. Time resolved magnetometry measurements made by our Academic Alliance Partnership with Prof. Victor Acosta's group at UNM are discussed. We finish with new approaches to improve the sensitivity of near surface NV color centers using carbon implantation to increase the number of vacancies near a N layer.

2. INTEGRATION OF NANOMATERIALS ON DIAMOND NV PLATFORM

To serve as a platform for materials investigation, NVs in diamond must be brought in close proximity with a material. With commercially available diamonds with lateral dimensions from 2 mm to 4 mm and thickness of 0.5 mm, this can be accomplished by either placing a diamond onto a material (i.e. by placing a diamond on a patterned Si substrate) [7], or by placing the material onto the diamond (i.e. dispersing nanoparticles on a diamond). The crystallographic orientation of the diamond substrate determines the 4 orientational directions of the NVs in the lattice. The experiments described in this report are performed on <100> diamonds from Element Six.

NVs in diamond can be incorporated into the growth as N impurities in CVD or HPHT optical grades (1-100 ppm N), or optimized layer of NVs can be implanted into very low impurity (<5 ppb N). For implanted diamonds, the depth of the NV layers is the primary factor in determining the length scale of the magnetometry. N can be implanted with a single energy to form a thin layer of N in the diamond, or for better signal, N can be implanted with multiple energies to approximate a uniform layer. Using the simulation software Stopping Range of Ions in Materials (SRIM) and a fitting procedure, we have designed uniform N layers for sensing experiments [8]. After implantation, a high temperature vacuum anneal activates NVs and reduces damage from the ion implant.

Conducting materials and metal films may need to be integrated for a number of reasons including reducing the optical transmission, magnetometry of a conducting quantum material or studying

NMR of metallic film. When depositing metal films on diamond with shallow NVs, the photoluminescence is reduced, possibly due to band bending leading to non-PL states such as NV+. By including a thin insulating layer, the photoluminescence can be increased.

2.1. Nanoparticle integration with diamond

To prepare for magnetometry measurements on SPIONs, we first investigated approaches that allowed us to deposit a high density of single nanoparticles on the surface of diamond in a controllable manner. We use a drop-cast technique where nanoparticles in hexane are deposited onto diamond using a pipet. The nanoparticles are coated in an oleic acid surfactant that enables them to be suspended in the hexane solution. A wicking method is needed to avoid a "coffee stain" pattern for a more homogeneous deposit. A typical method is wicking with a disposable wiper (Kimwipe) or putting on enough solution to break the surface tension, so the SPION solution overflows, allowing the solution to dry more homogeneously in both methods. One successful approach is to flip the diamond 90 degrees on its edge after placing 8 µL of solution on top to achieve a homogeneous deposition. To investigate the surface density of nanoparticles on the diamond, we drop-cast SPIONs using a range of dilutions. Serial dilution was performed to dilute the SPION solution with hexane by factors of two, resulting in eight solutions ranging from 1 mg/mL to 1/128 mg/mL, which were deposited using the wiping method described above. The entire procedure was repeated on to obtain a second set of eight diamonds.

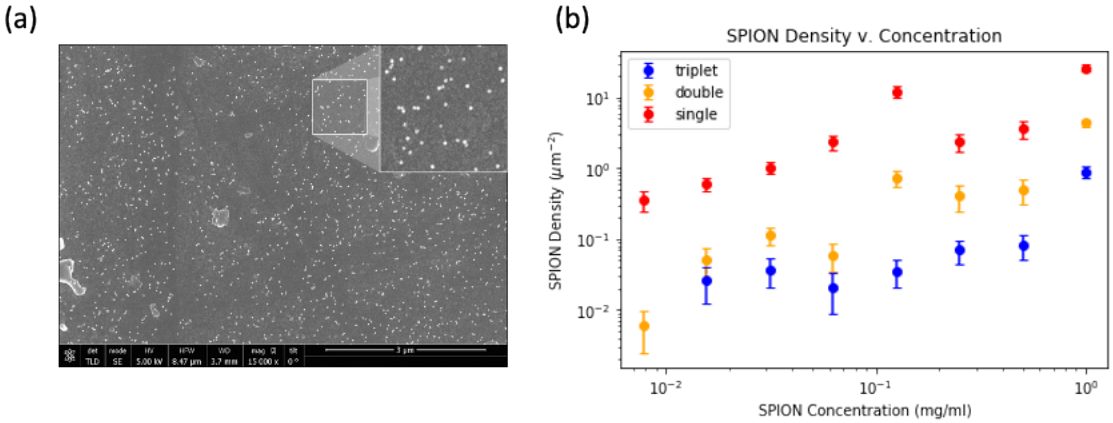

Figure 2 (a) SEM of 22 nm iron oxide nanoparticles on diamond for 1 mg/ml SPION concentration. (b) Surface density of single, double and triple groupings of nanoparticles for initial concentration nanoparticle solution.

After preparing diamonds with iron oxide nanoparticles on the surface, SEM image were taken of the resulting nanoparticle distributions. An example of an image of the diamond with nanoparticles is shown in Figure 2 with a magnified region shown in the upper right. The bright disks are individual 22 nm iron oxide nanoparticles. Care was taken to minimize charging on these images by coating the diamond with a 5 nm layer of chromium. In the image, isolated nanoparticles are observed, but there are also pairs of nanoparticles, triples of nanoparticles and larger clumps that can form. Nanoparticles in close proximity will interact, and likely change the magnetic measurements. To assess the density and connectivity of nanoparticles for deposition conditions, open computer vision software was used to automatically determine the location and connectivity of the nanoparticles in SEM images taken for 8 different initial concentrations of SPIONs in hexane. The results are show in the right graph of Figure 2 (a) SEM of 22 nm iron oxide nanoparticles on diamond for 1 mg/ml SPION concentration. (b) Surface density of single, double and triple

groupings of nanoparticles for initial concentration nanoparticle solution. In this experiment, the lowest concentration of $8x10^{-3}$ mg/ml of nanoparticles results in predominantly single nanoparticles on the surface. Increase the concentration increase the density of single nanoparticle (which will lead to higher detected signal), but also increase the number of interacting nanoparticles as well.

3. DC AND AC MAGNETOMETRY WITH NV COLOR CENTERS

3.1. Optically detected magnetic resonance

NV- centers in diamond have a spin 1 ground state with energy levels sensitive to the local magnetic field, and temperature. We have taken advantage of the magnetic field sensitivity to build a quantum sensing platform where we can image the dc magnetic fields and, using microwave pulsing techniques, measure magnetic resonance of materials on the surface of designer NV diamond structures.

At zero magnetic field, the $m_s=0$ level is split from the $m_s=\pm1$ levels by ~2.87 GHz. In the presence of a magnetic field, the energy levels are split by the Zeeman effect. For magnetometry, the spins must be initialized, manipulated, and read. Upon optical illumination, the $m_s=0$ state is initialized through non-radiative relaxation through the singlet channel. Application of microwaves at a frequency corresponding to the difference in energy levels can rotate the spin from $m_s=0$ to $m_s=1$ or $m_s=-1$ to $m_s=0$. The spin is read out optically by exciting with a 532 nm laser and measuring the photoluminescence from 650 nm and above. Optical relaxation to the $m_s=+1$ or $m_s=-1$ state are less bright than the $m_s=0$ relaxation. In order to establish and demonstrate magnetometry, we have built custom photoluminescence microscopes: three of which are connected to our homebuilt NV magnetic resonance spectrometers and are capable of measuring NV detected DC and AC fields up to GHz. These microscopes rely on single photon detection for the best PL sensitivity, and images are created by either scanning the sample or scanning the laser with a galvanometer 4f configuration. A fourth microscope has also assembled, demonstrated, and available to users for widefield DC imaging. Each of these microscopes is controlled by our custom python measurement software suite, pyscan.

3.2. T1 relaxometry

One approach to detecting the ac-magnetic response of a system of target spins is to adjust the magnetic field so that spin transitions in the target system coincide with spin transitions in the NVs. For free electron spins with g=2, the energy levels of the NVs and target cross at a field of 513 G (Figure 3a). Other spin population will have addition energy level crossings. Measurement of changes in the NV spin lifetime (T1) at these coincidences reveals information about this local spin environment [9,10]. The transition energy between the $m_s=\pm1$ and the $m_s=0$ states--which can be read out optically--can be tuned by varying an external magnetic field with a Zeeman response. When the energy splitting is in resonance with a local electromagnetic field, these energies interact with the NVs to shorten the lifetime of the polarized spin state back to thermal equilibrium. The longitudinal decay time, T1, can be measured through a polarization-relaxation experiment which swept over the NV resonant frequency yields information about the local fields.

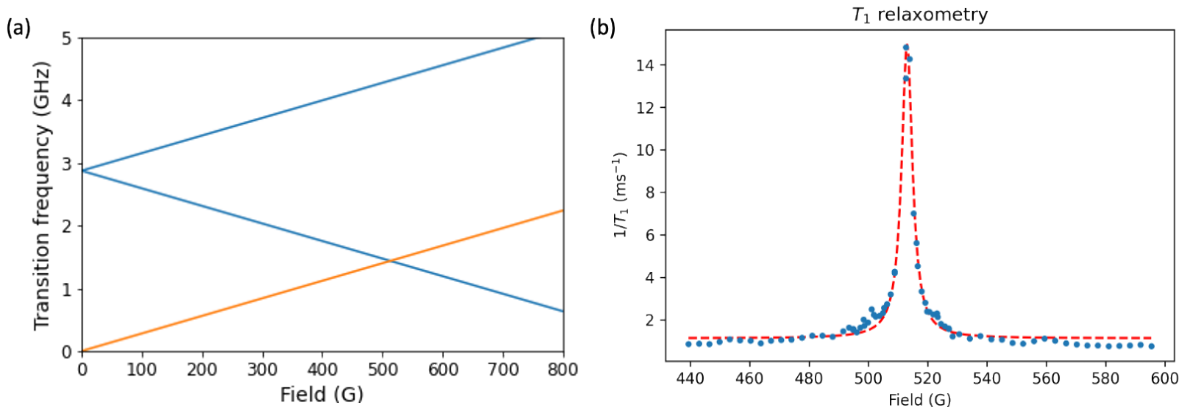

Figure 3 (a) Transition frequencies for NV- (blue) and g=2 electron spin (orange). (b) Inverse relaxation time of the NV spin. The peak is due to coincidence of g=2 background spins in bare diamond.

T1 relaxometry measurements for bare diamond are shown in Figure 3b. The peak at 513 G indicates excess relaxation due to nearby background spins with g=2. T1 relaxometry measurements with nanoparticles do not reveal any additional features beyond the main central g=2 spin peak. While this approach allows a passive detection of nearby spins by measuring NV relaxation times, a more direct approach for using NV centers in diamond to detect spins is discussed in the next section.

3.3. Double electron-electron resonance

In double electron-electron resonance experiments, electron spins in the spin 1 NV- and in the target population are controlled separately with two microwave signals. The first microwave signal controls the NV for ac-magnetometry and the second signal rotates nearby spins. These experiments have been used to measure concentrations of spin defects in diamond such as P1 centers (neutral charged substitutional N) [11]. In diamond materials, there are many other defects that lead to electronics states in addition to the NV centers. P1 centers are N sites substituted for C in the lattice. There are NV centers that are mis-aligned with the magnetic field. There can also be charges defects associated with vacancies or di-vacancies.

In this approach, two microwave signals are applied to device through the sample microwave stripline. One frequency is used to control the electron states in the NV, and the other is used to control the electron spin of the electron population under study. First, ODMR is measured on the NVs to determine the first microwave frequency. The initialization time for polarizing the NV spin to m_s=0 is determined. Microwave pulses of varying length are applied to the NV population to measure the Rabi frequency and set the times for pi and pi/2 pulses on the NVs. A Hahn-echo sequence is used on the NV centers in the diamond to find T2 and the optimal delay times. T1 is also measured to determine the reset time between pulse sequences. After the information on the NV operation has been collected, the pulse duration is varied for the second microwave signal to determine the rotation times of the target spin population. This is done for each feature in the DEER signal, and the target spins are inverted in the first part of the Hahn echo sequence [11]. If the second frequency is resonant with a population of target spins, a change in the photoluminescence is detected.

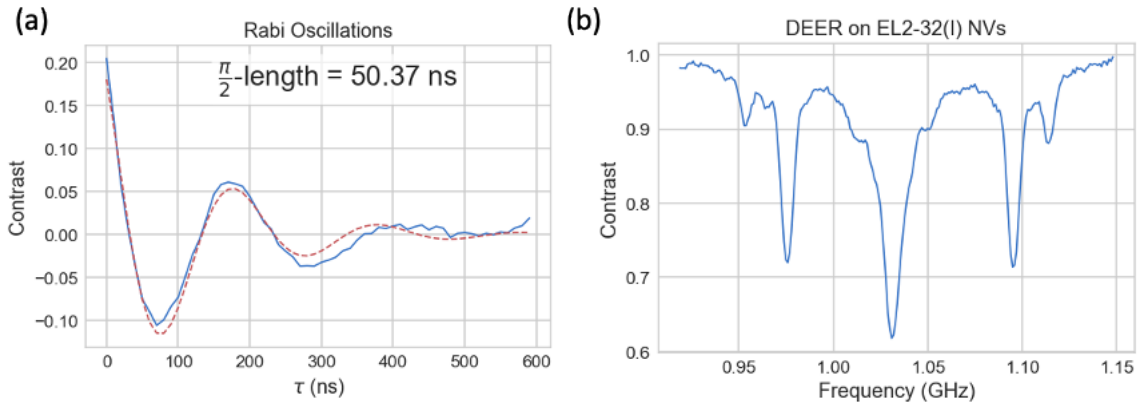

Figure 4 (a) Rabi oscillations of P1 central peak at 1.03 GHz. (b) DEER measurement showing P1 spectra in an electronics grade diamond with a 4 keV N implant and 100 ppm peak N density.

DEER measurements for an electronics grade diamond with an NV layer 6 nm below the surface are shown in Figure 4. The plot on the left shows Rabi oscillations for the second microwave frequency at 1.03 GHz. In this case, the target spins are a magnetic defect where single nitrogen atoms substitute for carbon in the lattice. These are also called P1 centers. The P1 spectra has 5 peaks in the DEER spectra due to the combination of electron spin ½ and hyperfine coupling with nuclear spin 1. These measurements can be used to directly determine the concentration of P1, NV- and NV0 defects in diamond [11]. In the future we will also explore DEER for measuring spin resonance of nanomaterials and quantum materials in close proximity to the diamond platform.

3.4. Impact of broad ESR linewidth on NV measurements

SPION spins align along an easy axis due to their anisotropic crystal structure and its paramagnetic response. However, in the absence of a magnetic field, the parallel and antiparallel orientations along this axis are equally energetically favorable, and at room temperature for sufficiently small SPIONs, the spin will flip along the easy axis with a mean flip time given by the Neel relaxation time [12] $\tau_N = \tau_0 \exp(KV/k_BT)$ where K is the magnetic anisotropy, V the volume, kB Boltzmann constant and T the temperature. Neel relaxation time measurements were performed by Prof. Victor Acosta with our Academic Alliance Partnership and are shown Section 3.5. A magnetic field will favor one orientation to the other with the relation [13, 14] $U = KV \sin^2(\theta) - \mu H \cos(\theta - \Psi)$. The SPIONs in bulk display superparamagnetic behavior, as one orientation is favored in the presence of a magnetic field, yielding a bulk ferromagnetic response, while when the thermal energy surpasses the magnetic potential energy, the SPIONs flip often enough that the bulk response is small, and the individual response is also small for measurements much longer than the Neel relaxation time. Because SPIONs are so small (e.g., 22-nm diameter), their bulk properties have been studied with fruitful results--however, their individual dynamics are not well understood. Specifically, we aimed to measure the spin response of single SPIONs and their interactions with each other.

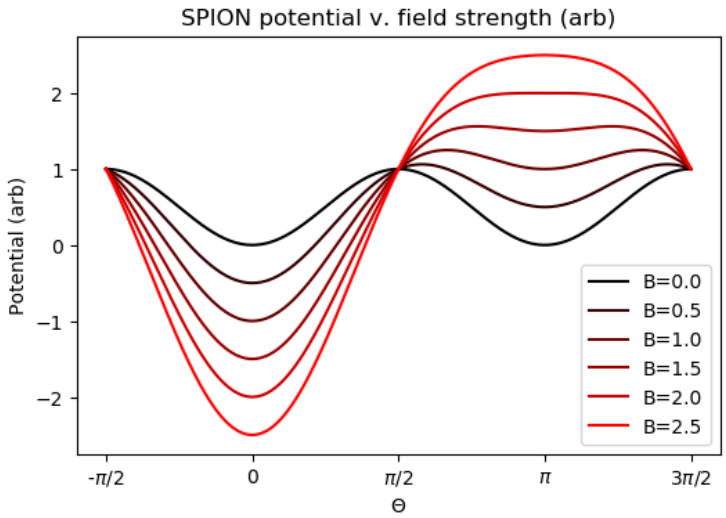

Figure 5 Low energy states parallel and antiparallel to the easy axis (θ=0) are equally energetically favorable, until an external magnetic field is applied.}

There are two noise spectra of interest with SPIONs: the ESR spectrum, and the spectral density. The spectral density is a measure of the Neel relaxation time, and the ESR spectrum gives information about the electron resonances within the SPION. By tuning the SPION density on the diamond surface, we should be able to measure single SPIONs if their signal is strong enough, or various densities of SPIONs otherwise. The width of the ESR spectrum could yield information about how the SPIONs interact with each other, and with low enough SPION concentration we might see several ESR peaks, indicating that interactions remove the SPION degeneracy.

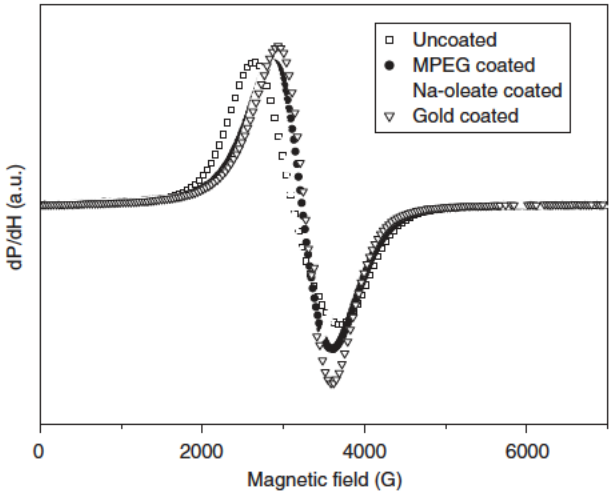

Figure 6 ESR of an ensemble of iron oxide nanoparticles from [15] for coated and uncoated nanoparticles.

In this project we successfully set up NV magnetometry, demonstrated in widefield and single-point modes, designed and characterized a microwave delivery device, developed several nanomaterial integration techniques with SEM calibration, characterized SPIONs, and detected ESR signals. However, the spectral density and ESR signals will be quite small for SPIONs. The ensemble ESR resonance shown in Figure 6 spans a full width half maximum of 550 G, implying that the SPION

signal would be spread to cover this entire frequency range. While the width of the ESR resonance might scale with the magnetic field, so that at the resonant NV field it would span 90 G, this wide range still results in considerable reduction of the measured signal. For reference, g=2 surface spins on a bare diamond measured using T1 relaxometry in Figure 3 had an amplitude of 14 ms^{-1} and a full width half max of approximately 4 G; a comparable signal spread over 550 G FWHM would reduce the signal to 0.16 ms^{-1}, which would be difficult to detect and require a lot of averaging in an already long experiment. Finally, the signal overlaps with the g=2 surface spin population in Figure 3; the magnitude of the background signal is dependent on the diamond preparation, and will overwhelm a small signal from SPIONs.

Despite this limitation, there is hope for using NV measurements to detect ESR in SPIONs. The ESR spectrum in Figure 6 is broad, but this may be because the traditional ESR technique is limited to measuring ensembles of SPIONs. A thin layer of SPIONs covering the diamond might have a more narrow ESR line, as SPION interactions may be the cause of significant broadening. If interactions play a significant role, the tradeoff between connected particles and nanoparticle density discussed in Section 2.1 are important. Second, the amplitude of the SPION signal was not observed, and the signal strength combined with any of the effects above may be enough to make the signal measurable. The suggested next steps would be to obtain measurements for multilayer SPIONs, monolayer SPIONs, and low-density SPIONs to optimize the signal at a SPION density which is not too sparse as to give too little signal, and not too dense as to give too wide an ESR spectrum. Once these limits are established, one could measure multiple SPION densities with the developed deposition methods and examine the ESR linewidth and shape as a function of density. To address whether the surface chemistry is unreliable, T1 would be measured on both sides of the diamond NV surface, then again measured with SPIONs deposited on one side of the same surface, and finally measured when the SPIONs are washed off. The present project has accomplished each of these procedures, short of T1 and DEER measurements on each side of the diamond.

3.5. Time Resolved Magnetic Microscopy: Academic Alliance Partnership

Through an Academic Alliance partnership with Victor Acosta's group at the University of New Mexico, the magnetic moment lifetimes of superparamagnetic nanoparticles were studied. The time scale for relaxation of magnetization in nanoparticles depends on both the nanoparticle size and on the local environment. Some of the applications of SPIONs considered for this work include early cancer detection and tagging of non-magnetic objects.

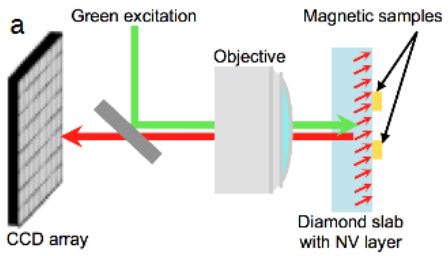

Figure 7 CCD imaging approach of magnetic nanoparticles

Diamond substrates with NV layers were coated with SPIONs. As described in Section 3.1, the local magnetic field was imaged using a combination of optically detected magnetic resonance techniques combined with CCD imaging of the resulting photoluminescence. By varying the microwave frequency and observing minima in the PL, the magnetic field can be determined.

Capturing the PL with a CCD camera allows for rapid magnetic field measurement of multiple nanoparticles.

Time resolved images taken using the approach shown in Figure 8. The SPIONs are polarized with a 300 gauss field, and then the magnetic field is reduced to the measurement value of -15 gauss. The magnetic field is measured over the entire field of view of the CCD (Figure 8, middle) several times a second. The relaxation of the magnetic field over 30 seconds is shown for regions 0, 7 and 23 in Figure 8, right.

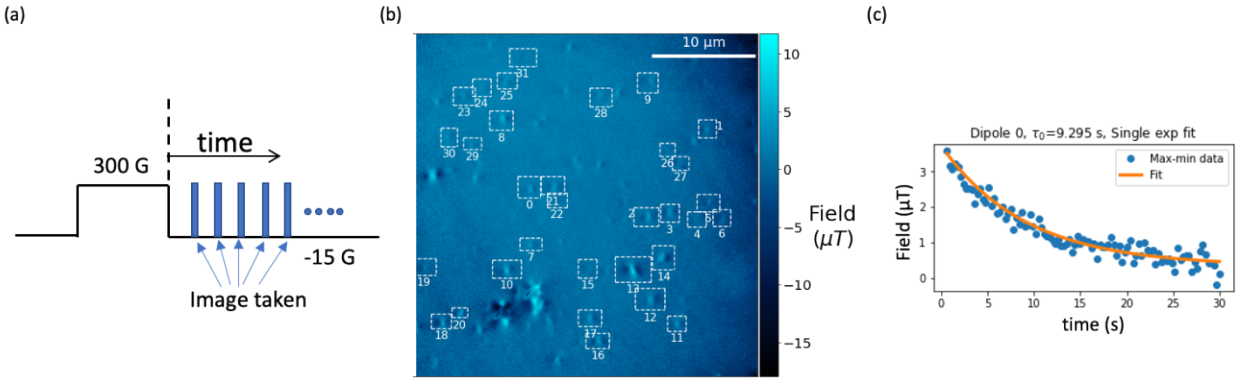

Figure 8 Relaxation measurements for SPIONs. (a) The particles are initially polarized at 300 G, and then the field is lowered to the measurement value of -15 G. A sequence of images (blue markers) is taken to determine the field. (b) CCD image of the second scan. SPIONs are denoted with white dashed boxes. (c) Time dependence of "Dipole 0" (labeled in b) magnetic field relaxation.

The Academic Alliance partnership accelerated progress on the "Quantum Sensed Electron Spin Resonance Discovery Platform" LDRD. Both UNM and Sandia benefitted from exchange of technical information by attending group meetings, working with UNM students and direct discussions.

4. EFFICIENT FORMATION OF NV COLOR CENTERS IN DIAMOND

The depth of NV centers in a diamond used for sensing the magnetic field of a nearby material depends on the type of magnetometry being performed. For dc measurements with micron-scale resolution, the NV layers can be thick so that the signals are large [16]. For NMR and ESR experiments, the NV sensing layer needs to be quite shallow (20 nm or less). The challenge with shallow NV implants is that the activation of NVs can be very low close to the surface. One approach to improve the formation of the nitrogen-vacancy centers is to generate extra vacancies that can diffuse near a nitrogen containing layer to promote the formation of NV centers [17].

4.1. Hot implant of carbon for excess vacancies

Implantation of carbon into electronics grade diamond is one approach to introduce many vacancies for every carbon implanted without unwanted additional elements in the carbon diamond lattice. Using electronics grade diamond (5 ppb N), we implant 100 ppm nitrogen with 4 keV. The N implant creates some vacancies, and after an 800 C / 1100 C anneal, about 1% of the N join with a vacancy to form NVs [18]. The samples are cleaned and T1, T2, T2* and the photoluminescence are characterized. Additional vacancies are created using a 46 keV carbon implant at the Tandem accelerator at Sandia's Ion Beam Laboratory. For this experiment, the diamond is then loaded into and half is masked for direct comparison of the effect of hot implantation.

The goal is to introduce vacancies without permanently damaging the diamond (graphitization). There are several competing effects to make good NV sensors. First, converting N to NV reduces the P1 center background, and can increase the coherence time for the NVs. This improves the sensitivity. Second, reducing the number of N changes the local band effects near the NV, and that can convert NV- to NV0. This decreases the number of useable NVs. Measurements will guide the optimal implant choice.

To calculate the depth and number of vacancies for the 46 keV carbon implant, we use SRIM (Stopping and Range of Ions in Matter). For each carbon ion, approximately 117 vacancies are generated. The vacancies are distributed from 0 to ~70 nm, and peak at 55 nm. The 4 keV N peaks at 6.3 nm below the surface, so the extra vacancies from the carbon surround the N layer. For a carbon fluence of 1.5 x 10^{13} carbon/cm^2, the peak vacancy density is 2.3 x 10^{20}. This is below the graphitization threshold of 10^{21}-10^{22} vacancies / cm^3.

4.2. Improving efficiency of NV formation

Initial photoluminescence measurements are shown in Figure 9. Diamonds were implanted with 1.0 x 10^{13} carbon/cm^2 (sample EL2-31) and 1.5 x 10^{13} carbon/cm^2 (sample EL2-32). EL2-31 was at 800 C for 6 min. EL2-32 was at 800 C for 120 min. The photoluminescence of the diamond looks artificially bright in the bottom of both images due to the sample mount. We averaged the PL in the implanted and un-implanted regime, and found the ratio of PL intensity for the implanted vs un-implanted sides is 1.95 and 0.86 for EL2-31 and EL2-32 respectively.

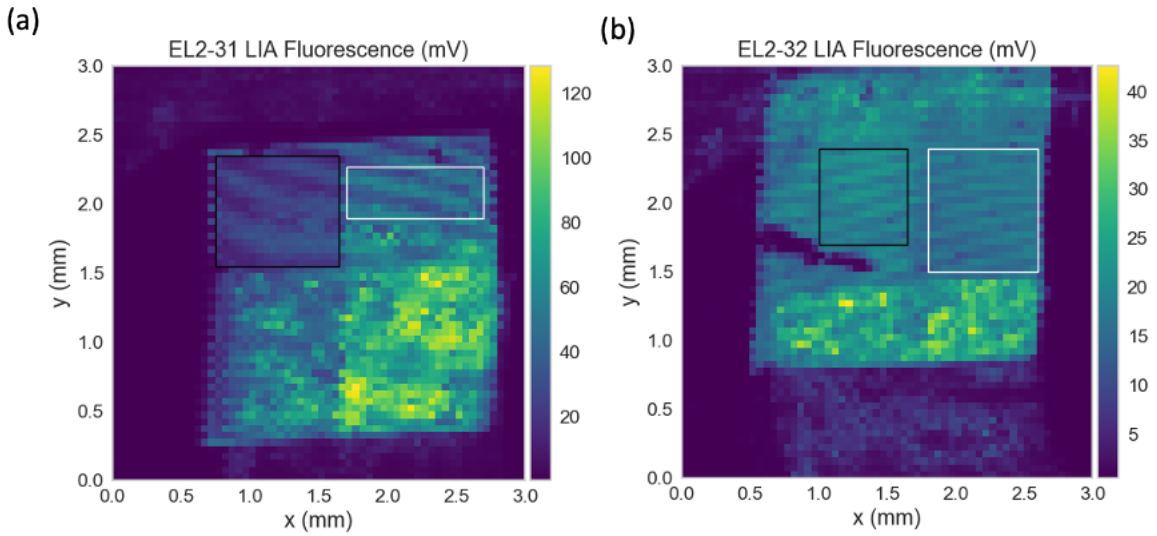

Figure 9 Photoluminescence of diamonds with 800 C carbon implant. (a) EL2-31 where ratio of PL intensity for the hot-implanted to non-implanted sides is 1.95. (b) EL2-32 where ratio of PL intensity for the hot-implanted to non-implanted sides is 0.86.

5. CONCLUSIONS

In this report we described our progress on building a quantum sensing electron spin resonance platform using NV color centers in diamond. Diamond substrates with shallow NV layers were designed and prepared to enable DC and AC magnetometry. Techniques for drop-casting nanoparticles in solution on diamond substrates were used to place SPIONs on the surface of diamond. We investigated the nanoparticle coverage and connectivity using automated software analysis with open computer vision libraries. DC magnetic fields were measured with NV color

centers using an optically detected magnetic resonance. The AC magnetic response of the local environment was detected using T1 relaxometry and DEER measurements. One approach to improve the sensitivity of the diamond NV platform is to improve the formation efficiency of NVs in diamond. We are using carbon implantation to increase the number of vacancies and allow more background N to convert to NVs. The diamond NV platform developed in this project provides a combination of good magnetic field sensitivity and high spatial resolution and will be used for future investigations of nanomaterials and quantum materials.

REFERENCES

1 Huber, D. L. Synthesis, Properties, and Applications of Iron Nanoparticles. Small 1, 482–501 (2005).
2 Degen, C. L., Reinhard, F. and Cappellaro, P., "Quantum sensing", Reviews of Modern Physics 89 (3), 035002 (2017).
3 Casola, F., van der Sar, T. and Yacoby, A., "Probing condensed matter physics with magnetometry based on nitrogen-vacancy centres in diamond", Nature Reviews Materials 3 (1), 17088 (2018).
4 Noginov, M. M., Noginova, N., Amponsah, O., Bah, R., Rakhimov, R. and Atsarkin, V. A., "Magnetic resonance in iron oxide nanoparticles: Quantum features and effect of size", Journal of Magnetism and Magnetic Materials 320 (18), 2228-2232 (2008).
5 John Watt, et al., Non-volatile iron carbonyls as versatile precursors for the synthesis of iron-containing nanoparticles. Nanoscale 9, 6632–6637 (2017).
6 Noginov, M. M., Noginova, N., Amponsah, O., Bah, R., Rakhimov, R. and Atsarkin, V. A., "Magnetic resonance in iron oxide nanoparticles: Quantum features and effect of size", Journal of Magnetism and Magnetic Materials 320 (18), 2228-2232 (2008).
7 Kehayias, P., Bussmann, E., Lu, T.-M. and Mounce, A. M., "A physically unclonable function using NV diamond magnetometry and micromagnet arrays", Journal of Applied Physics 127 (20), 203904 (2020).
8 Kehayias, P., Henshaw, J., Saleh Ziabari, M., Titze, M., Bielejec, E., Lilly, M. P. and Mounce, A. M., "A fitting algorithm for optimizing ion implantation energies and fluences", Nuclear Instruments and Methods in Physics Research Section B: Beam Interactions with Materials and Atoms 500-501, 52-56 (2021).
9 Tetienne, J. P., Hingant, T., Rondin, L., Cavaillès, A., Mayer, L., Dantelle, G., Gacoin, T., Wrachtrup, J., Roch, J. F. and Jacques, V., "Spin relaxometry of single nitrogen-vacancy defects in diamond nanocrystals for magnetic noise sensing", Physical Review B **87** (23), 235436 (2013).
10 Hall, L. T., Kehayias, P., Simpson, D. A., Jarmola, A., Stacey, A., Budker, D. and Hollenberg, L. C. L., "Detection of nanoscale electron spin resonance spectra demonstrated using nitrogen-vacancy centre probes in diamond", Nature Communications 7 (1), 10211 (2016).
11 Li, S., Zheng, H., Peng, Z., Kamiya, M., Niki, T., Stepanov, V., Jarmola, A., Shimizu, Y., Takahashi, S., Wickenbrock, A. and Budker, D., "Determination of local defect density in diamond by double electron-electron resonance", arXiv:2104.00744.
12 Ludwig, F., Heim, E. and Schilling, M., "Characterization of superparamagnetic nanoparticles by analyzing the magnetization and relaxation dynamics using fluxgate magnetometers", Journal of Applied Physics 101 (11), 113909 (2007).
13 Chantrell, R. W., Walmsley, N., Gore, J. and Maylin, M., "Calculations of the susceptibility of interacting superparamagnetic particles", Physical Review B 63 (2), 024410 (2000).
14 Deissler, R. J., Wu, Y. and Martens, M. A., "Dependence of Brownian and Néel relaxation times on magnetic field strength", Medical Physics 41 (1), 012301 (2014).
15 Koseoglu, Y., Yildiz, F., Kim, D., Muhammed, M. & Aktas, B. in Nanostructured Magnetic Materials and their Applications 303-312 (Springer, 2004).
16 Kehayias, P., Bussmann, E., Lu, T.-M. and Mounce, A. M., "A physically unclonable function using NV diamond magnetometry and micromagnet arrays", Journal of Applied Physics 127 (20), 203904 (2020).
17 Schwartz, J., Michaelides, P., Weis, C. D. and Schenkel, T., "In situoptimization of co-implantation and substrate temperature conditions for nitrogen-vacancy center formation in single-crystal diamonds", New Journal of Physics 13 (3), 035022 (2011).
18 Nebel, C. E., in Semiconductors and Semimetals, edited by C. E. Nebel, I. Aharonovich, N. Mizuochi and M. Hatano (Elsevier, 2020), Vol. 103, pp. 73-136.

DISTRIBUTION

Email—Internal

Name	Org.	Sandia Email Address
Michael Lilly	01882	mplilly@sandia.gov
Technical Library	01977	sanddocs@sandia.gov

This page left blank

This page left blank

Sandia National Laboratories

Sandia National Laboratories is a multimission laboratory managed and operated by National Technology & Engineering Solutions of Sandia LLC, a wholly owned subsidiary of Honeywell International Inc. for the U.S. Department of Energy's National Nuclear Security Administration under contract DE-NA0003525.